

Targeting Podoplanin for the Treatment of Osteosarcoma



Ai Takemoto¹, Satoshi Takagi¹, Takao Ukaji¹, Nobuhiko Gyobu², Mamoru Kakino², Miho Takami¹, Asami Kobayashi¹, Marie Lebel¹, Tokuchi Kawaguchi³, Minoru Sugawara³, Kazue Tsuji-Takayama², Kenji Ichihara², Yuki Funauchi⁴, Keisuke Ae⁴, Seiichi Matsumoto⁵, Yoshiya Sugiura⁶, Kengo Takeuchi^{6,7,8}, Tetsuo Noda⁹, Ryohei Katayama¹, and Naoya Fujita¹⁰

ABSTRACT

Purpose: Osteosarcoma, the most common bone malignancy in children, has a poor prognosis, especially when the tumor metastasizes to the lungs. Therefore, novel therapeutic strategies targeting both proliferation and metastasis of osteosarcoma are required. Podoplanin (PDPN) is expressed by various tumors and is associated with tumor-induced platelet activation via its interaction with C-type lectin-like receptor 2 (CLEC-2) on platelets. We previously found that PDPN contributed to osteosarcoma growth and metastasis through platelet activation; thus, in this study, we developed an anti-PDPN humanized antibody and evaluated its effect on osteosarcoma growth and metastasis.

Experimental Design: Nine osteosarcoma cell lines and two osteosarcoma patient-derived cells were collected, and we evaluated the efficacy of the anti-PDPN-neutralizing antibody PG4D2 and the humanized anti-PDPN antibody AP201, which had IgG4 framework region. The antitumor and antimetastasis effect of PG4D2

and AP201 were examined *in vitro* and *in vivo*. In addition, growth signaling by the interaction between PDPN and CLEC-2 was analyzed using phospho-RTK (receptor tyrosine kinase) array, growth assay, or immunoblot analysis under the suppression of RTKs by knockout and inhibitor treatment.

Results: We observed that PG4D2 treatment significantly suppressed tumor growth and pulmonary metastasis in osteosarcoma xenograft models highly expressing PDPN. The contribution of PDGFR activation by activated platelet releasates to osteosarcoma cell proliferation was confirmed, and the humanized antibody, AP201, suppressed *in vivo* osteosarcoma growth and metastasis without significant adverse events.

Conclusions: Targeting PDPN with a neutralizing antibody against PDPN–CLEC-2 without antibody-dependent cell-mediated cytotoxicity and complement-dependent cytotoxicity is a novel therapeutic strategy for PDPN-positive osteosarcoma.

Introduction

Osteosarcoma is rare but is the most common primary malignant bone tumor in children and adolescents. A 2016 survey indicated that there are 20,000 to 30,000 patients with osteosarcoma per year worldwide. Standard treatments for osteosarcoma include chemotherapy and surgery, which are effective to a degree (1). In a recent report, the 5-year survival rate for patients with osteosarcoma increased to 60% to 70%; however, that for patients with osteosarcoma and metastasis is about 20% (2). Therefore, effective therapies for osteosarcoma that target the mechanism underlying osteosarcoma metastasis, which is probably related to the tumor microenvironment, in addition to the standard combination chemotherapy, are needed (3).

Podoplanin (PDPN) is a potential therapeutic target in osteosarcoma because PDPN is frequently highly expressed in clinical osteosarcoma samples (4–7). A correlation between high PDPN

expression and poor prognosis has been observed (5–7). Moreover, high PDPN expression from metastases, rather than from the primary lesion, has been reported (5–8). PDPN is a type I transmembrane sialoglycoprotein that is frequently upregulated in several tumor types (5, 9–14), and its expression imparts tumor cells the ability to activate platelets by interacting with C-type lectin-like receptor 2 (CLEC-2) expressed on the platelet surface (15–17). The binding of PDPN to CLEC-2 leads to downstream signaling activation in platelets through Syk/Src phosphorylation and results in the activation and aggregation of platelets (16, 18, 19). Activated platelets secrete various growth factors and cytokines that are deposited within alpha-granules in platelets. Platelet–tumor cell clusters are then trapped in the microvasculature in the lung or other organs, which may become a trigger for metastasis. Factors secreted from platelets, such as TGFβ, lysophosphatidic acid (LPA), or others, may change the morphology and characteristics of cancer

¹Division of Experimental Chemotherapy, Cancer Chemotherapy Center, Japanese Foundation for Cancer Research (JFCR), Koto-ku, Tokyo, Japan.

²API Co., Ltd., Kanosakuradacho, Gifu-shi, Gifu, Japan. ³Project for Development of Genomics-based Cancer Medicine, Cancer Precision Medicine Center, JFCR, Koto-ku, Tokyo, Japan. ⁴Department of Orthopedic Oncology, Cancer Institute Hospital, JFCR, Koto-ku, Tokyo, Japan. ⁵Sarcoma Center, Cancer Institute Hospital, JFCR, Koto-ku, Tokyo, Japan. ⁶Division of Pathology, Cancer Institute, JFCR, Koto-ku, Tokyo, Japan. ⁷Department of Pathology, Cancer Institute Hospital, JFCR, Koto-ku, Tokyo, Japan. ⁸Pathology Project for Molecular Targets, Cancer Institute, JFCR, Koto-ku, Tokyo, Japan. ⁹Cancer Institute, JFCR, Koto-ku, Tokyo, Japan. ¹⁰Cancer Chemotherapy Center, JFCR, Koto-ku, Tokyo, Japan.

Note: Supplementary data for this article are available at Clinical Cancer Research Online (<http://clincancerres.aacrjournals.org/>).

Current address for K. Tsuji-Takayama: URA division, Hiroshima University, Hiroshima City, Hiroshima, Japan; and current address for Y. Sugiura: Department of Pathology, Toho University Sakura Medical Center, Sakura City, Chiba, Japan.

Corresponding Author: Naoya Fujita, Cancer Chemotherapy Center, Japanese Foundation for Cancer Research, 3-8-31, Ariake, Koto-ku, Tokyo 135-8550, Japan. Phone: 81-3-3570-0468; Fax: 81-3-3570-0484; E-mail: naoya.fujita@jfcrc.or.jp

Clin Cancer Res 2022;28:2633–45

doi: 10.1158/1078-0432.CCR-21-4509

This open access article is distributed under Creative Commons Attribution-NonCommercial-NoDerivatives License 4.0 International (CC BY-NC-ND).

©2022 The Authors; Published by the American Association for Cancer Research

Translational Relevance

Osteosarcoma often affects the bones or joints, especially in children and young adults. Standard therapies for osteosarcoma are chemotherapy and surgery. The 5-year survival rate of patients with osteosarcoma is 60% to 70%; however, that of patients with metastasis, mostly to the lungs, is reduced to about 20%. Thus, new therapeutic strategies to inhibit the metastasis and progression of osteosarcoma are warranted. Podoplanin (PDPN) is expressed by various tumors and induces platelet activation by binding with CLEC-2 expressed on the platelets. In this study, we found that PDPN is expressed in more than half of osteosarcoma. Then, we developed a humanized anti-PDPN antibody, AP201, that can neutralize PDPN–CLEC-2 binding, and demonstrated the inhibition of both the progression and metastasis of osteosarcoma without antibody-dependent cell-mediated cytotoxicity or complement-dependent cytotoxicity *in vivo*.

cells, such as inducing epithelial–mesenchymal transition (EMT) in the epithelial cancer or increasing cell migration/invasion (20, 21).

As PDPN is highly expressed from various tumor types and contributes to tumor-induced platelet activation, the PDPN–CLEC-2 interaction could be a promising target for inhibiting tumor metastasis as well as growth in PDPN-positive tumors. Currently, many anti-PDPN mAbs have been developed in our and other laboratories, and some of these antibodies have been reported to exhibit neutralizing activity against the PDPN–CLEC-2 interaction (17, 22–25). In particular, our previously developed mouse anti-human PDPN antibody, PG4D2, exhibited strong neutralizing activity as it recognizes the region around PLAG4, which is the most crucial area for PDPN to bind to CLEC-2 (25). In addition, PG4D2 administration suppressed the hematogenous metastasis of tail vein-injected human PDPN-transfected Chinese hamster ovary (CHO) cells (25). These PG4D2-mediated antimetastatic effects were also observed in bladder squamous cell carcinoma UM-UC-5 cells, which endogenously express human PDPN (26). In addition, PG4D2 suppressed tumor growth *in vivo* partially by inhibiting the secretion of growth factors and cytokines from activated platelets. PG4D2 may have partially exhibited antitumor activity owing to its antibody-dependent cell-mediated cytotoxicity (ADCC) and complement-dependent cytotoxicity (CDC), as a subtype of PG4D2 is mouse IgG2a. However, ADCC/CDC activity may not be required for PDPN-targeting therapy as we confirmed that another anti-PDPN antibody, MS-1, of mouse IgG2a subtype with PLAG3 domain-binding capability reduced the growth of PDPN-positive lung squamous PC-10 cells xenografted into immunodeficient NOD/SCID mice (24). The underlying mechanism of the promotion of PC-10 cell growth by platelets could be explained as follows: the infiltrated platelets leak into the tumor tissue from immature tumor blood vessels and are activated through the interaction between PDPN on tumor cells and CLEC-2 on platelets. Then, multiple released growth factors, such as EGF or PDGF, may promote PC-10 cell growth (27).

Here, we evaluated PDPN expression in osteosarcoma tumor tissues and in originally developed patient-derived as well as publicly available osteosarcoma cell lines. We then tested antitumor and antimetastasis activity of anti-PDPN antibody PG4D2 in osteosarcoma tumor xenografts expressing different levels of PDPN. In addition, we examined how PDPN-mediated platelet activation induced osteosarcoma growth. For the clinical application, we developed a humanized

PG4D2, AP201 antibody, of the human IgG4 subtype harboring no ADCC/CDC activity, and evaluated the antitumor and antimetastatic activity in a PDPN-positive osteosarcoma model. Our results strongly indicate that our PDPN-neutralizing antibody is a promising therapeutic agent for osteosarcoma treatment.

Materials and Methods

IHC staining

Bone and cartilage tissue microarray was purchased from Bio-max (T262a: <https://www.biomax.us/T262a>, T263: <https://www.biomax.us/T263>, T264a: <https://www.biomax.us/T264a>), and clinical specimens were retrieved from patients with osteosarcoma treated at the Cancer Institute Hospital in the Japanese Foundation for Cancer Research (JFCR) with informed consent following the protocol approval by the Institutional Review Board (IRB) committee of JFCR. Information on the patient from whom Sa-xeno-147-P0 was retrieved: a 11-year-old male, pathologically diagnosed with fibroblastic type grade 1 conventional osteosarcoma, with lung metastasis 7 months after postoperative chemotherapy. Information on the patient from whom GCB53-G3 was retrieved: a 13-year-old male, pathologically diagnosed with conventional giant cell-rich grade 4 osteosarcoma, with no recurrence or metastasis after postoperative chemotherapy. The clinical specimens were formalin-fixed and paraffin-embedded (FFPE); then, representative surgical tissue sections from the paraffin-embedded blocks were extracted for IHC staining using anti-human PDPN antibodies (PG4D2; in-house developed mouse anti-human PDPN mAb and D2-40; Dako #M3619) and hematoxylin–eosin staining.

Cell lines

Human osteosarcoma cell lines SJS-1 (RRID: CVCL_1697), MG63 (CVCL_0426), HOS (CVCL_0312), Saos-2, 143B (CVCL_2270), MNNG/HOS Cl #5 (CVCL_0439), and KHOS/NP (CVCL_2546), were purchased from ATCC, NOS-10 (CVCL_4663) from RIKEN Bioresource Research Center; and NY (CVCL_1613) from JCRB Cell Bank. They were tested *Mycoplasma* free by vendors and used for experiments within a short period of culture from thawing. If cell stocks were over about five times of passage, cells were authenticated by short tandem repeat (STR) analysis. Sa-xeno-147-P0 and GCB53-G3 cell lines established from clinical specimens of patients with osteosarcoma at JFCR Hospital were determined to be similar to the clinical sample and the primary culture via STR analysis. The culture method is written in Supplementary Materials and Methods. PDPN- or PDGFR α / β -knocked out SJS-1 or NOS-10 cells were developed using the Dharmacon Edit-R CRISPR Cas9 Gene Engineering System in which Cas9 expression plasmid vector (*puroR+*), *trans*-activating CRISPR RNA, and targeting or nontargeting CRISPR RNA were transfected together into cells using DharmaFECT Duo Transfection Reagent and selection with puromycin.

Animals

NSG (NOD.Cg-Prkdc^{scid}Il2rg^{tm1Wjl}/SzJ), NOD-SCID (NOD.CB17-Prkdc^{scid}/J), and SCID beige (CB17.Cg-Prkdc^{scid}Lysf^{bsg-J}/CrIcrIj), ICR (CrI:CD1(ICR)) mice were purchased from Charles River Laboratories, Inc. *Pdpr*^{KI/KI} C57BL/6N mice were developed and maintained in our laboratory (28). All animal procedures were performed following the protocol approved by the Committee for the Use and Care of Experimental Animals of JFCR in accordance with relevant guidelines and regulations.

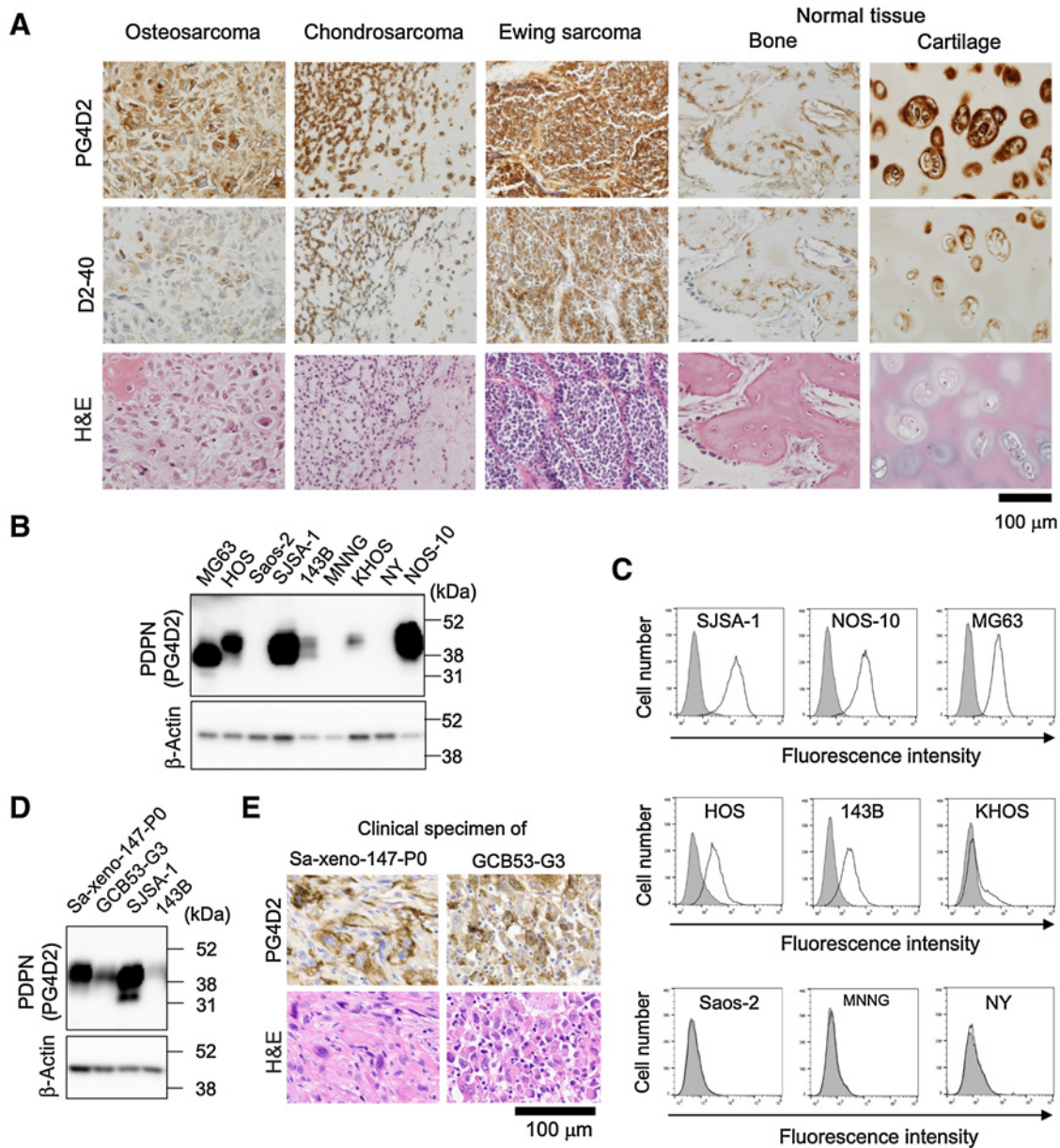


Figure 1. PDPN expression in osteosarcoma clinical samples and cell lines. **A**, IHC analysis of PDPN expression was performed with mouse anti-human PDPN mAbs (PG4D2 or D2-40) and hematoxylin and eosin (H&E) staining against tissue microarrays containing 10 osteosarcoma, seven chondrosarcoma, three Ewing sarcoma, and normal tissue (Bio-max). Typical samples from each type were selected and are shown. **B**, PDPN expression in osteosarcoma cell lines available from public cell banks was detected by immunoblotting with the indicated antibodies. **C**, Cell surface PDPN expression was detected by flow cytometry using an anti-PDPN antibody, D2-40. **D**, PDPN expression in patient-derived osteosarcoma cells was detected by immunoblotting with the indicated antibodies. **E**, IHC analysis to detect PDPN expression using PG4D2 and H&E staining was performed against clinical osteosarcoma specimens, which were used for the establishment of Sa-xeno-147-P0 and GCB53-G3 cell lines. Scale bars, 100 μ m.

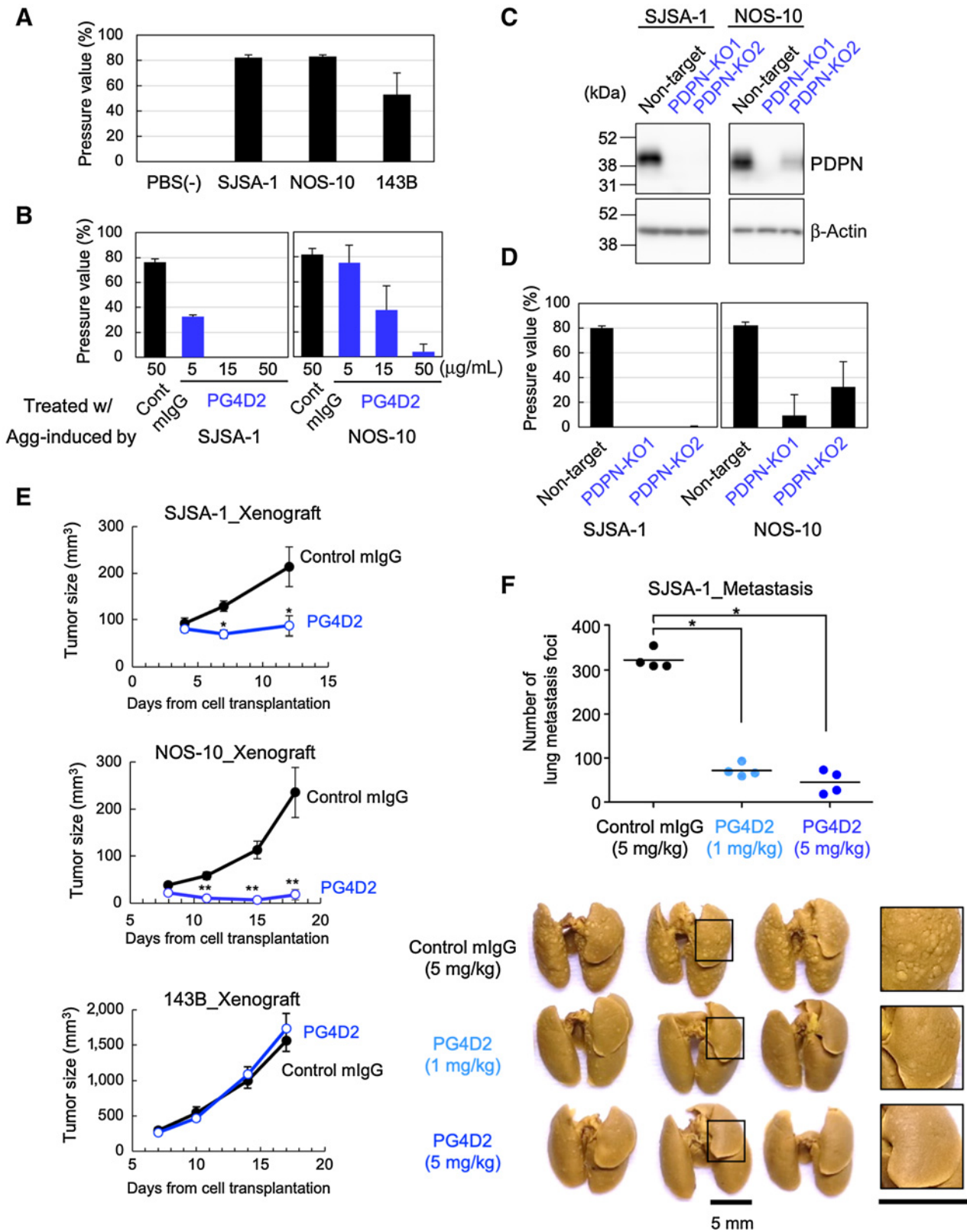
Development and maintenance of patient-derived osteosarcoma cells

Clinical specimens were obtained from patients with osteosarcoma at the Cancer Institute Hospital in JFCR with informed consent as per the protocol approved by the IRB committee of the JFCR. The osteosarcoma clinical samples were subcutaneously engrafted into NSG or NOD/SCID mice to obtain patient-derived xenograft (PDX) models. Cell lines were established from

PDX model or directly from a clinical sample as written in Supplementary Materials and Methods.

Human whole blood aggregation assay

Whole blood aggregation induced by osteosarcoma tumor cells was monitored using the WBA-Carna system. A blood sample was collected in a tube with 0.38% sodium citrate from healthy volunteers with informed consent and was dispensed into 200 μ L aliquots per assay



cuvette with a stirrer bar. Then, 10 μL of osteosarcoma cells (5×10^5 in PBS) was added and induced aggregation was measured after 15 minutes of incubation. To detect the inhibition of aggregation by anti-PDPN Ab, a titrated concentration series of 10 μL of Ab (final concentration: 5, 15, or 50 $\mu\text{g}/\text{mL}$) was added to the blood sample, and after 2 minutes of incubation, the osteosarcoma cells were added. After incubation for 15 minutes, platelet aggregation was detected by the system.

Preparation of washed human platelets and platelet aggregation assay

Human whole blood was collected in a tube with 0.38% of sodium citrate and washed platelets were prepared as described in a study by Takagi and colleagues (29). In the assay, washed platelets were adjusted to $1 \times 10^9/\text{mL}$, SJSA-1 cells (5×10^4 cells) were added to the platelet suspension (200 μL), and platelet aggregation was monitored using an aggregometer (MCM HEMA TRACER 313M; SSR Engineering). After 30 minutes of incubation, the platelet-aggregated or nonaggregated reactants were collected to obtain platelet-activated or control supernatants by centrifugation.

Growth assay

Growing cells were seeded into a 96-well plate and co-cultured for 4 days with platelet-activated/control supernatants or PDGF-BB ligands (50 ng/mL, R & D systems). For inhibitor treatment, sunitinib or gefitinib (1 $\mu\text{mol}/\text{L}$) were added. Cell growth was measured using the Premix WST-1 cell proliferation (TaKaRa) or the CellTiter Glo assay (Promega). For treatment with the platelet supernatant, the WST-1 assay was used.

Evaluation of the antitumor efficacy of antibody using xenograft and lung metastasis models

For xenograft models, SJSA-1 (5×10^6), NOS-10 (7×10^6), or 143B (5×10^6) prepared as suspensions in 100 μL of Hank's Balanced Salt Solution (HBSS; Wako)/mouse were subcutaneously injected into the right flank of SCID beige mice, and antibody administration by tail vein injection twice a week was initiated on day 1 or 3 after tumor cell injection. Long (L) and short diameters (W) of the growing xenograft tumors were measured, and the tumor volume was calculated approximately using the following formula: $\frac{1}{2} \times L \times W^2$. For hematogenous metastasis models, intravenous administration of antibody to SCID beige mice was performed one day before tumor cell injection; for SJSA-1 patient-derived cell lines (4×10^5), Sa-xeno-147-P0 (1×10^6) cells were prepared as a suspension in 200 μL of HBSS/mouse. After the proper period depending on the model, the mice were sacrificed for lung metastasis dissection. Lungs were excised, picric acid-stained, and the number of metastatic foci on the lung surface was counted.

Study approvals

All patients with osteosarcoma provided informed consent and agreed to the use of surgically resected specimens for research purposes prior to surgery. Blood for the platelet aggregation assay was provided from healthy volunteers who signed informed consent. This study using clinical specimens and blood was approved by the IRB of the JFCR following Ethical Guidelines for Medical and Biological Research Involving Human Subjects issued by the Japanese government. All *in vivo* studies on mice were conducted in line with protocols approved by the Committee for the Use and Care of Experimental Animals of JFCR following guidelines related to animal experiments issued by the Japanese government.

Statistical analysis

The Kruskal–Wallis test was performed to determine the statistical significance of the *in vivo* results. Some *in vitro* results were analyzed using the Mann–Whitney U or t tests. Significant P values are shown as $*P < 0.05$ and $**P < 0.01$. All statistical tests were two sided.

Data availability statement

The data obtained in this study are available upon reasonable request from the corresponding author.

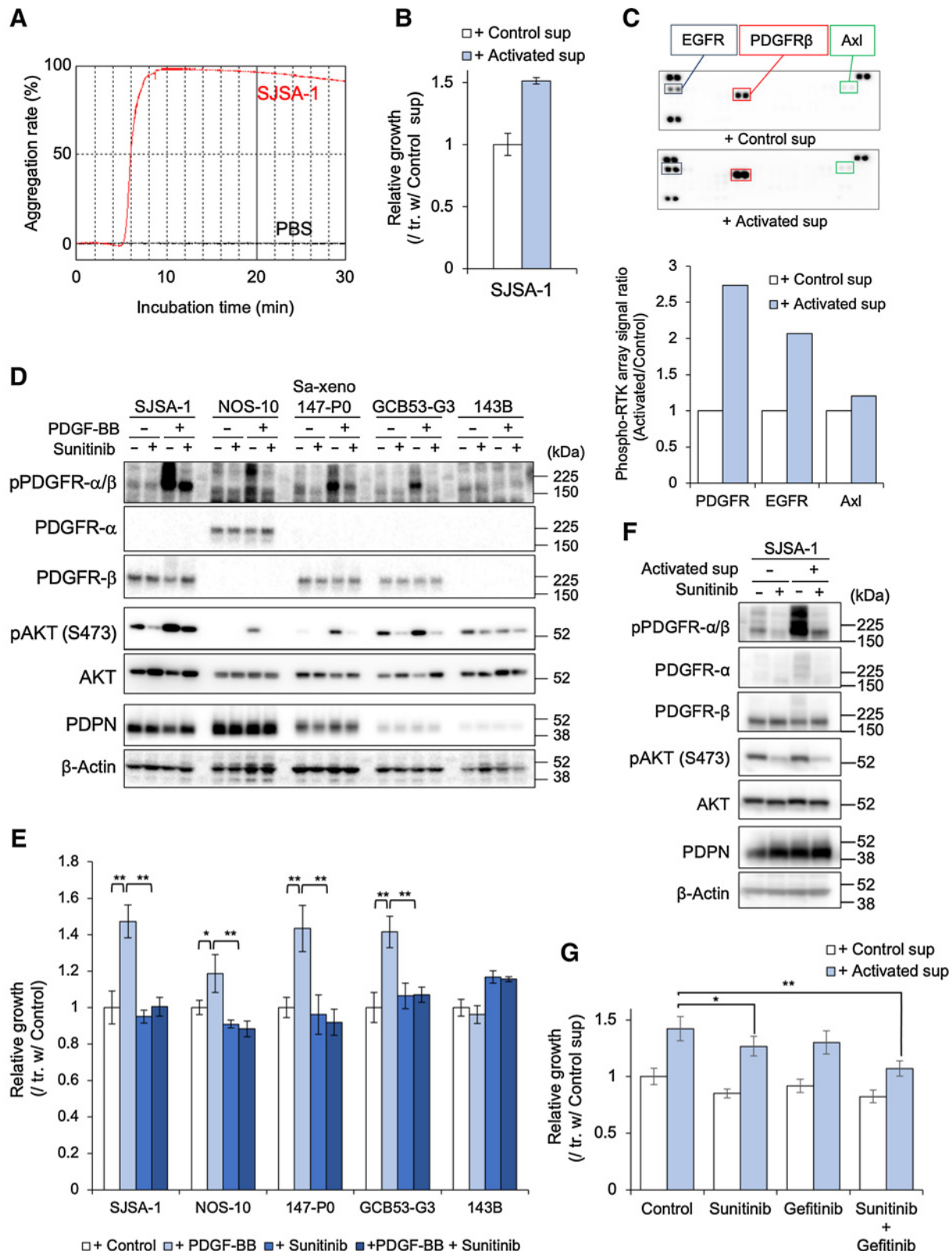
Results

PDPN overexpression in human osteosarcoma and other sarcomas

Osteosarcoma has been reported to highly express PDPN on its surface and to show poor prognosis accompanied with pulmonary metastasis, and treatment strategies for osteosarcoma remain limited (7, 30). First, we examined the expression of PDPN in FFPE specimens of osteosarcoma, chondrosarcoma, and Ewing sarcoma using the commercially available mouse anti-human PDPN antibody D2-40 and the mouse anti-human PDPN antibody PG4D2, which recognizes the PLAG4 domain and was developed by us (25). As shown in **Fig. 1A**, the staining patterns of D2-40 antibody and PG4D2 were similar and concordant to a certain degree, although the staining intensity with PG4D2 was higher than that with D2-40 antibody. Staining with PG4D2 suggested that eight of 10 osteosarcoma, six of seven chondrosarcomas, and one of three Ewing sarcoma samples were positive for PDPN expression (**Fig. 1A**). Notably, three of eight osteosarcoma samples expressed PDPN highly. At higher magnifications, PDPN was detected on the plasma membrane and intracellularly in tumor cells. Second, we investigated PDPN expression in human osteosarcoma cell lines obtained from public cell banks. On immunoblotting (**Fig. 1B**) and flow cytometry (**Fig. 1C**), six cell

Figure 2.

PDPN-dependent platelet aggregation, tumor growth, and metastasis in osteosarcoma. **A**, Platelet aggregation–inducing activity of osteosarcoma cells (5×10^5 / 0.2 mL / assay); SJSA-1, NOS-10, and 143B cells were evaluated using human whole blood by an aggregometry (WBA-Carna). In the assay, measured and shown pressure values (%) are regarded as the aggregation level. The average \pm SD ($n = 4$) is shown. **B**, A platelet aggregation assay was performed in the high PDPN-expressing osteosarcoma cell lines SJSA-1 and NOS-10 in the presence of the indicated concentrations of PG4D2 (5, 15, or 50 $\mu\text{g}/\text{mL}$) in comparison with control mouse IgG2a (50 $\mu\text{g}/\text{mL}$). **C**, PDPN expression level in the established PDPN knockout (PDPN-KO1 or PDPN-KO2) SJSA-1 and NOS-10 cells was examined by immunoblotting with PG4D2 and anti- β -actin antibody. **D**, The impact of PDPN-KO on the platelet aggregation activity of osteosarcoma cells was evaluated using a human whole blood platelet aggregation assay. **E**, High PDPN-expressing cell lines SJSA-1 and NOS-10, or the low PDPN-expressing 143B cell line, were subcutaneously inoculated into immunodeficient SCID beige mice (5×10^6 , 7×10^6 , or 5×10^6 /mouse) and treated with PG4D2 (5 mg/kg) or control mouse IgG (5 mg/kg) twice a week. Tumor growth was measured at the indicated timepoints and average \pm SE was shown. **F**, Antimetastatic activity of PG4D2 on pulmonary metastasis of osteosarcoma. PG4D2 (1 or 5 mg/kg) or control mouse IgG (5 mg/kg) was intravenously injected one day before SJSA-1 cell intravenous injection (4×10^5). After 20 days, the mice were euthanized and the number of metastatic foci on the lung surface was counted after picric acid staining. The representative pictures of lungs and the magnified images surrounded by boxes are shown (graph demonstrating the number of metastatic foci; top, lung photos; bottom, bars; 5 mm). Statistical analyses of the *in vivo* data were performed using the Kruskal–Wallis test. *, $P < 0.05$; **, $P < 0.01$.



lines of nine (67%) were found to exhibit PDPN positivity. Among the osteosarcoma cell lines, SJSA-1 and NOS-10 highly expressed PDPN on their cell surfaces, and the PDPN expression levels of these cells were similar to that in normal lung tissue known to be the highest expression in the mouse body (Supplementary Fig. S1; ref. 28). We also assessed PDPN expression in osteosarcoma cell lines obtained from samples surgically resected from patients with osteosarcoma after obtaining informed consent (Sa-xeno-147-P0 and GCB53-G3; Fig. 1D). The original tumor specimens of Sa-xeno-147-P0 and GCB53-G3 were positive for PDPN on IHC staining with PG4D2 (Fig. 1E).

Anti-PDPN-neutralizing antibody PG4D2 inhibited platelet activation, tumor growth, and metastasis of osteosarcoma

We previously reported that the growth of the osteosarcoma cell line MG63 was upregulated by platelet-secreted growth factors, such as PDGF, during osteosarcoma-induced platelet aggregation (29). As the PLAG4 domain of PDPN is mainly associated with PDPN-CLEC-2 binding and leads PDPN-induced platelet aggregation, targeting the PLAG4 domain could inhibit osteosarcoma growth; however, this was not completely evaluated in our previous study (29). Our previously developed anti-PDPN antibody PG4D2 had high affinity to PDPN and neutralizing activity against PDPN-CLEC-2 binding (25). In this study, we evaluated the antitumor activity of PG4D2 on PDPN-expressing osteosarcoma. We first evaluated the platelet aggregation activity of osteosarcoma cells and its dependency on PDPN. High PDPN-expressing osteosarcoma cells (SJSA-1 and NOS-10) exhibited higher platelet aggregation activity than low PDPN-expressing 143B cells (Fig. 2A). PDPN-expressing osteosarcoma cells induced platelet aggregation, and the expression was suppressed following PG4D2 treatment in a dose-dependent manner (Fig. 2B). To further confirm the importance of PDPN on platelet activation in SJSA-1 and NOS-10 osteosarcoma cells, we introduced guide RNAs against PDPN with Cas9 and developed PDPN knockout cells (Fig. 2C). As expected, almost no platelet aggregation was observed in PDPN knockout SJSA-1 and NOS-10 cells (Fig. 2D). Notably, PDPN knockout in SJSA-1 cells did not affect their growth *in vitro* (Supplementary Fig. S2B).

To investigate the contribution of PDPN-dependent platelet aggregation to osteosarcoma tumor growth *in vivo*, high PDPN-expressing SJSA-1 and NOS-10 cells or low PDPN-expressing 143B cells were subcutaneously inoculated into SCID beige mice lacking B-cell, T-cell, and natural killer-cell activity, but sustained the platelets and coagulation activity. PG4D2 was intravenously administered at 5 mg/kg twice per week, which leads a blood PG4D2 concentration similar to the concentration we used to suppress osteosarcoma-induced platelet aggregation in the *in vitro* platelet aggregation assay. PG4D2 markedly inhibited the *in vivo* growth

of the xenografted tumor's SJSA-1 and NOS-10 cells (Fig. 2E); however, it did not prevent the growth of low PDPN-expressing 143B cells. These results suggest that the *in vivo* growth of high PDPN-expressing SJSA-1 and NOS-10 cells, but not low PDPN-expressing 143B cells, depends on PDPN. Next, we examined the inhibitory effects of PG4D2 on the hematogenous metastasis of SJSA-1 cells. SJSA-1 cells were intravenously injected into the tail vein and pulmonary metastasis was monitored after 1 month. In this metastasis model, the administration of a single dose of PG4D2 at 1 or 5 mg/kg once a day before SJSA-1 injection significantly reduced the formation of metastatic foci in the lungs (Fig. 2F). The suppressive effect of PG4D2 administration on hematogenous metastasis was also observed when a patient-derived osteosarcoma cell line, Sa-xeno-147-P0, was intravenously injected into SCID beige mice (Supplementary Fig. S3A). The Sa-xeno-147-P0 cell-induced platelet aggregation was also suppressed by PG4D2 *in vitro* (Supplementary Fig. S3B). Thus, the antitumor and antimetastatic abilities of PG4D2 *in vivo* might not be supported by the ADCC activity of PG4D2.

PDGFR and EGFR ligand secretion from PDPN-activated platelets contributes to osteosarcoma cell growth

PDPN-expressing SJSA-1 cells showed marked growth inhibition following anti-PDPN-neutralizing antibody PG4D2 treatment, suggesting that the interaction of PDPN with SJSA-1 and platelet surface CLEC-2 plays a critical role in tumor growth *in vivo*. When SJSA-1 cells and washed human platelets were incubated, platelet activation and aggregation were immediately induced (Fig. 3A). When SJSA-1 cells were incubated with SJSA-1-treated activated platelet supernatants, cell growth was promoted to 1.5 times that of control nonactivated platelet supernatant-treated SJSA-1 cells (Fig. 3B). Phospho-RTK (receptor tyrosine kinase) array analysis using SJSA-1 cell lysates treated with control or activated platelet supernatant revealed that PDGFR β , EGFR, and Axl were activated after the addition of activated platelet supernatants (Fig. 3C). PDGFR β is effectively activated by its ligand, PDGF-BB. Thus, three commercially available and two patient-derived primary osteosarcoma cell lines were treated with PDGF-BB. As a result, phosphorylation of PDGFRs and downstream phospho-AKT were upregulated by PDGF-BB treatment. Treatment with the PDGFR inhibitor, sunitinib, clearly decreased phospho-PDGFR and phospho-AKT levels in these PDGFR-expressing cells. As 143B cells did not express PDGFRs, no phospho-PDGFRs or phospho-AKTs were observed after PDGF-BB treatment (Fig. 3D). The growth of four PDGFR-expressing osteosarcoma cell lines was consistently promoted by PDGF-BB treatment, and treatment with sunitinib ameliorated the promotion of growth by PDGF-BB (Fig. 3E). In contrast, 143B cells without PDGFR expression did not respond to PDGF-BB treatment

Figure 3.

PDPN-mediated platelet aggregation and resultant PDGFR activation induce growth promotion in OS. **A**, SJSA-1 cells or control PBS were incubated with washed human platelets, and platelet aggregation was monitored using an aggregometer. **B**, Supernatant collected from nonactivated (incubated with PBS; Control sup) or activated platelets (coincubated with SJSA-1; Activated sup) was added to naïve SJSA-1 cells and incubated for 4 days. The relative cell growth was estimated using the WST-1 assay. **C**, A phospho-RTK array was performed using SJSA-1 cell lysate that had been incubated with nonactivated or activated platelet supernatants. The relative signal intensity of phosphorylated PDGFR, EGFR, or Axl is shown as a bar graph. **D**, The indicated osteosarcoma cell lines were treated with or without 10 ng/mL of PDGF-BB in the presence of control DMSO or the PDGFR inhibitor sunitinib (1 μ mol/L). After 15 minutes of incubation, the cell lysate was collected and analyzed by immunoblotting with the indicated antibodies. **E**, The indicated osteosarcoma cell lines were incubated with 50 ng/mL of PDGF-BB with or without 1 μ mol/L of sunitinib for 4 days. The cell growth was measured using a WST-1 assay. The relative cell growth to that of cells treated with control is shown. **F**, SJSA-1 cells were incubated with Activated sup or Control sup shown in **B** in the presence or absence of sunitinib (1 μ mol/L). After 15 minutes of incubation, the cell lysates were collected and analyzed by immunoblotting with the indicated antibodies. **G**, SJSA-1 cells were incubated with Activated sup or Control sup in the presence of control DMSO, sunitinib, and/or gefitinib. After 4 days of incubation, cell growth was measured by the WST-1 assay. PDGFR inhibitor and EGFR inhibitor stopped the growth promoting activity of the activated sup-treated SJSA-1. Average \pm SD ($n = 5$) were shown. Statistical analyses of the data were performed using *t* test. *, $P < 0.05$; **, $P < 0.01$.

(Fig. 3E). Immunoblot analysis demonstrated that PDGFR was expressed in nine of 11 osteosarcoma cells used in this study (Supplementary Fig. S1). The addition of activated platelet supernatants significantly increased phospho-PDGFR levels, and sunitinib treatment completely inhibited the phospho-PDGFR level in SJSA-1 cells (Fig. 3F). When SJSA-1 cells were treated with activated platelet supernatant with or without sunitinib, the promotion of growth was partially halted, but treatment with sunitinib together with EGFR inhibitor, gefitinib, almost completely stopped the promotion of growth induced by the activated platelet supernatant (Fig. 3G). As sunitinib targets multiple kinases, such as VEGFR, RET, FLT3, and c-Kit, along with PDGFR, we performed similar experiments using other selective kinase inhibitors: CP-673451 and orantinib (31, 32). We found that PDGF stimulated growth of NOS-10 and SJSA-1 were both inhibited on administration of 30 nmol/L of CP-673451 or 300 nmol/L of orantinib (Supplementary Fig. S4). Three osteosarcoma cell lines, SJSA-1, Sa-xeno-143-P0, and GCB53-G3, expressed PDGFR β mainly. On the other hand, NOS-10 cells expressed PDGFR α (Fig. 3D; Supplementary Fig. S1). Therefore, we knocked out PDGFR β in SJSA-1 cells and PDGFR α in NOS-10 cells to evaluate the contribution of PDGFR to osteosarcoma cell growth (Supplementary Fig. S3). The growth rate in PDGFR-knockout cells did not show any change compared with that in parental NOS-10 or SJSA-1 cells (Supplementary Fig. S2B); however, we did observe compromised growth promotion by PDGF-BB (Supplementary Fig. S2C). These results suggest that high PDPN-expressing osteosarcoma cells activate platelets, and the resultant PDGFs, including PDGF or EGFR ligands, may promote osteosarcoma cell growth. Therefore, inhibition of PDPN-CLEC-2 binding mediated platelet activation upstream of this cascade, which might be a promising therapeutic strategy to treat patients with osteosarcoma.

Development of a humanized anti-PDPN antibody AP201

To further improve the PG4D2 for clinical application, we developed a humanized PG4D2 antibody, AP201. For humanization, we first sequenced the PG4D2 antibody and defined complementary determining regions (CDR) that function in direct binding to the antigen (see Supplementary Materials and Methods). The defined CDRs were then inserted into the framework regions (FR) of the human IgG4 subtype sequence selected from germline genes based on its homology to the PG4D2 (Fig. 4A and B). We chose a human IgG4 subtype lacking ADCC/CDC activity to reduce any unexpected adverse toxicity against PDPN-positive normal cells, such as type I alveolar cells in the lungs and podocytes in the kidney. There was limited information about the toxicity induced by the ADCC/CDC activity of PG4D2 targeting PDPN-expressing normal tissues in the early development stage of the humanized antibody. Recently, no acute toxicity was found in monkeys after a single high-dose administration of anti-monkey PDPN surrogate antibody (2F7; ref. 33).

We then checked combinations of PG4D2 CDR and germline genes and selected FR sequences with high homology to PG4D2 antibody as the heavy (H) and light (L) chains. We inserted several combinations of H and L chains into the pCHO 1.0 expression vector and stably transfected them into CHO cells (Fig. 4B). The released antibodies were collected and purified using protein A and ion-exchange columns (see Supplementary Materials and Methods). The purity of the humanized antibody was confirmed to be over 95% by SDS-PAGE, and the observed minor bands were related products, as they were detected by immunoblotting using an anti-human IgG4 antibody, and the epitope of AP201 antibody was confirmed to be exactly the same as

that of PG4D2 (Supplementary Fig. S5A and S5B). We screened antibodies showing sufficient binding activity to human PDPN and neutralizing activity against PDPN-CLEC-2 binding, and we selected one antibody named AP201 (Fig. 4C). AP201 exhibited high PDPN binding activity similar to the mouse-human chimeric antibody (chPG4D2) with CDRs and FRs that were the same as those of PG4D2 antibody. Surface plasmon resonance analysis revealed that the association rate constant (k_a) of AP201 was about 6.5×10^4 M/second, and the dissociation rate constant (k_d) failed to reach a value measurable by BiacoreX100 owing to the low-level dissociation (Fig. 4D). Thus, the precise equilibrium dissociation constant (K_D) value of AP201 could not be calculated; however, it was less than 0.3 nmol/L, a value that is almost the same as that of PG4D2 (25).

We next investigated ADCC and CDC activity (Fig. 4E and F). ADCC activity was monitored as Fc effector activity using Fc γ RIII α /NFAT luciferase reporter vector-transfected Jurkat and PDPN-positive target SJSA-1 cells. As SJSA-1 cells abundantly express EGFR, we used cetuximab, an anti-EGFR human IgG1 subtype antibody, as a positive control. We also used chimeric MS-1 antibody (chMS-1), a PLAG3-recognizing anti-human PDPN chimeric antibody of the human IgG1 subtype (24). AP201 did not exhibit a reporter signal, whereas cetuximab and chMS-1 exhibited ADCC activity (Fig. 4E), indicating that AP201 did not exhibit ADCC activity itself. We then examined CDC activity using an assay system that detects lactate dehydrogenase (LDH) release from lysed SJSA-1 cells in the presence of complements and antibodies. Compared with the PG4D2 of the mouse IgG2a subtype, AP201 of the human IgG4 subtype did not exhibit CDC activity (Fig. 4F). Thus, we developed AP201 as a human IgG4 subtype with no ADCC or CDC activity. We then compared the PDPN-neutralizing activity of AP201 with that of PG4D2. The inhibitory activity against PDPN binding to CLEC-2 was estimated using ELISA (Fig. 5A). The IC₅₀ values of the inhibitory activity were similar among AP201, PG4D2, and chPG4D2 (359.9, 357.8, and 404.6 ng/mL, respectively). In addition, the AP201-neutralizing activity of recombinant CLEC-2 binding to PDPN expressed on CHO cells was similar to that of PG4D2 (Fig. 5B and C). Moreover, AP201 suppressed SJSA-1-induced platelet aggregation similar to PG4D2 (Fig. 5D and E). Therefore, the neutralizing activity of humanized AP201 may be sufficient to inhibit tumor progression by suppressing PDPN-mediated platelet aggregation.

Humanized antibody AP201 exhibited antitumor and antimetastatic efficacy in a xenografted osteosarcoma model

Human OS SJSA-1 and NOS-10 cells were subcutaneously injected into the right flank of an immunodeficient SCID beige mouse. Treatment of the mouse with AP201 significantly suppressed the growth of SJSA-1 and NOS-10 xenografted tumors without body weight changes (Fig. 6A and B). Furthermore, one day before AP201 administration, the number of pulmonary metastases of SJSA-1 cells decreased (Fig. 6C). In addition, AP201 treatment markedly inhibited the lung metastasis of patient-derived Sa-xeno-147-P0 osteosarcoma cells (Fig. 6D). The antitumor and antimetastatic efficacies were similar to those of PG4D2 administration (Fig. 2E and F). AP201 did not exhibit ADCC/CDC activity (Fig. 4E and F) or suppress *in vitro* SJSA-1 cell growth (Supplementary Fig. S5C), suggesting that the ability of AP201 to neutralize PDPN function was associated with antitumor and antimetastatic abilities. In other words, PDPN-mediated platelet aggregation could partially contribute to the growth of osteosarcoma and might be a novel therapeutic target in osteosarcoma.

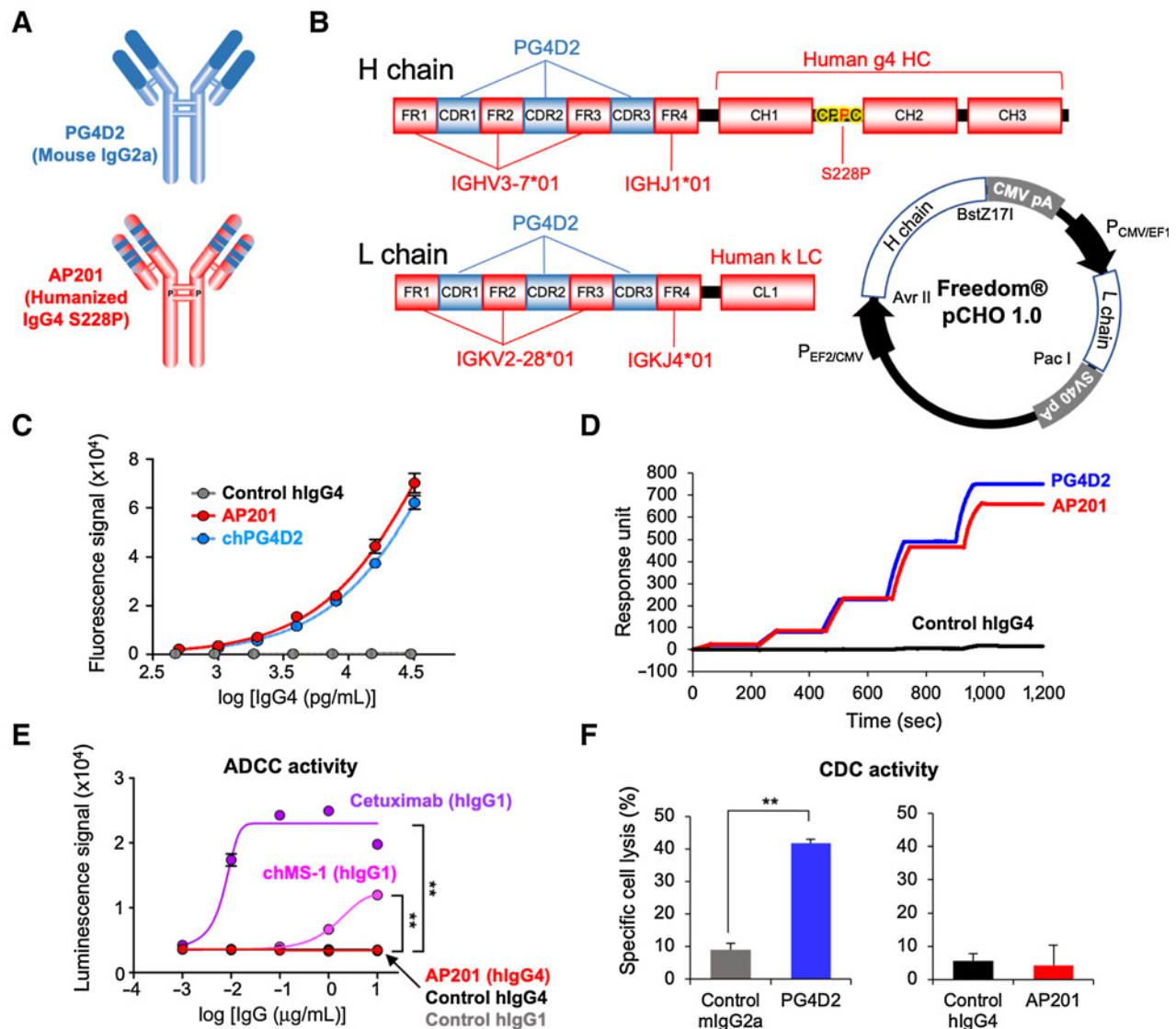


Figure 4. The humanization of PG4D2 to ADCC/CDC activity-deficient human IgG4 subtype. **A**, Schematic representation of PG4D2 (mouse IgG2a) and developed humanized AP201 (human IgG4). **B**, Schematic representation of the developed humanized AP201. CDR sequences of PG4D2 were defined (see Materials and Methods) and inserted into the selected FR sequences of human IgG4. To stabilize the developed human IgG4 holo-complex, serine 228 in the hinge region was replaced with proline (S228P). The heavy (H) and light (L) chains of the humanized AP201 and the expression vector integrating these sequences are indicated. **C**, The binding activity of control human IgG4 (hlgG4), AP201, or chimeric PG4D2 antibody (chPG4D2) (human IgG4 subtype) to human recombinant PDPN was measured by ELISA. **D**, Surface plasmon resonance analysis was performed using the Biacore X100 system with the human PDPN protein immobilized on the CM-5 tip. PG4D2, AP201, and its control hlgG4 were spiked, and the response was monitored. Equilibrium dissociation constants (K_D) of PG4D2 or AP201 on human PDPN were not calculated as the K_D values were less than the detectable limit in this system, 1×10^{-5} . **E**, ADCC activity of AP201 was measured using an ADCC reporter bioassay (Promega) and SJS-1 as the target cell and compared with that of human IgG1-like chimeric anti-PDPN antibody, chMS-1, anti-EGFR antibody cetuximab or control IgGs (control hlgG1 or hlgG4). **F**, CDC activity of PG4D2 or AP201 was analyzed using a baby rabbit complement and SJS-1 as the target cell. After 5.5 h of incubation, SJS-1 cell lyses were measured using the LDH-Go cytotoxicity assay.

Safety of AP201 administration

For the clinical development of AP201, we then performed safety tests using our previously developed human PDPN knock-in mice (*Pdpr*^{KI/KI} mice). PDPN is expressed in a broad range of normal organs and tissues, such as type I alveolar epithelial cells in the lungs and podocytes in the kidney, and is associated with development and homeostasis in some organs (34). However, we previously found that a high-dose single administration

(100 mg/kg) of 2F7 surrogate anti-monkey PDPN antibody harboring PG4D2-like neutralizing activity did not demonstrate acute toxicity in cynomolgus monkeys (33). Moreover, we confirmed that there was no toxicity or change in hematologic and biochemical parameters after repeated PG4D2 administration in *Pdpr*^{KI/KI} mice expressing human/mouse chimeric PDPN in which the mouse PLAG4 domain was replaced with the human homologous PLAG4 domain (28).

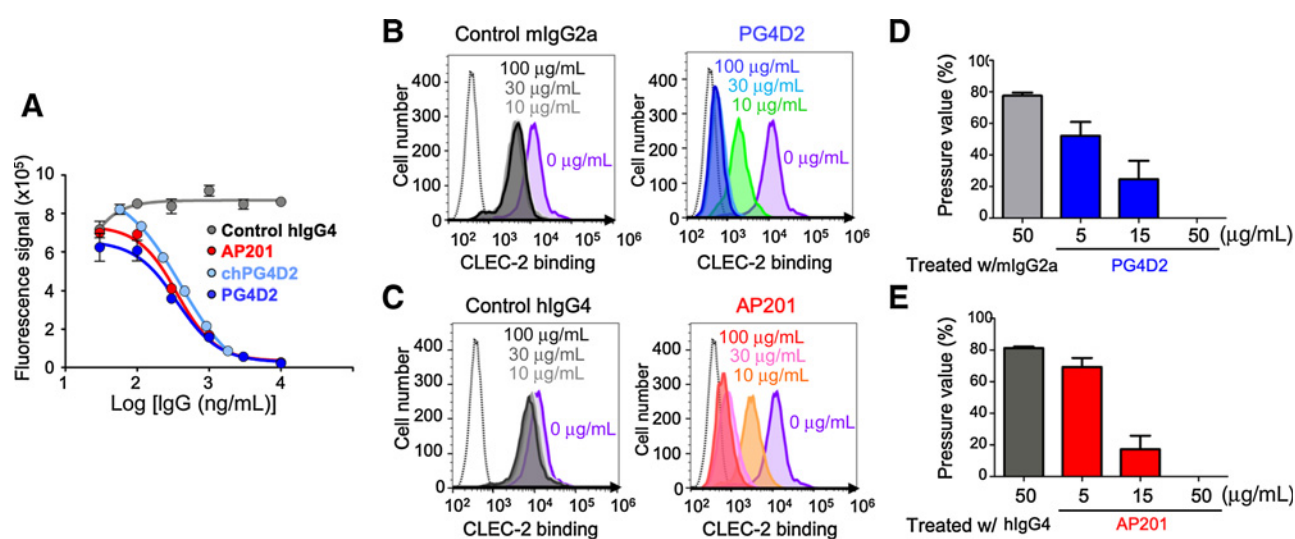


Figure 5.

The neutralizing activity of AP201 against PDPN-platelet binding and PDPN-induced platelet aggregation. **A**, The neutralizing activity of AP201, PG4D2, chimeric PG4D2 (chPG4D2), or control human IgG4 against PDPN-CLEC-2 interaction was evaluated using ELISA. The neutralizing activity of PG4D2 (**B**) and AP201 (**C**) against recombinant CLEC2-His₁₀ binding to CHO cells expressing human PDPN was confirmed by flow cytometry using Alexa Fluor 488-conjugated anti-penta-His antibody. Control mouse IgG2a and human IgG4 were also examined. The inhibitory effect of PG4D2 (**D**) or AP201 (**E**) against SJS-1-induced platelet aggregation was evaluated in human whole blood aggregometry using WBA-Carna. Titrated antibodies (5, 15, 50 µg/mL) or their control IgGs (50 µg/mL) were tested.

A high-dose single administration (50 mg/kg) of AP201 did not exhibit any sign of acute toxicity hematologically and histologically (Supplementary Tables S1 and S2; Supplementary Fig. S6). These results strongly indicated that PDPN targeting is a promising strategy for osteosarcoma therapy with low toxicity. Of note, half-life of the AP201 in the mouse was calculated as 14.56 days, which is sufficiently stable and similar to that of PG4D2.

Discussion

In this study, we found that PDPN is expressed in more than half of all surgically dissected osteosarcoma, chondrosarcoma, and Ewing sarcoma samples as well as multiple osteosarcoma cell lines that were examined. PDPN expressed on the cell surface in osteosarcoma contributed to PDPN-CLEC-2-mediated platelet aggregation and activation, resulting in tumor growth and metastasis through PDGFR or other signals induced by factors released by platelets. Our previously developed potent anti-human PDPN antibody, PG4D2 neutralized PDPN-CLEC-2 binding and inhibited PDPN-positive tumor growth and pulmonary metastasis. To further improve this antibody for clinical application, we developed a humanized anti-PDPN antibody, AP201. The affinity and neutralizing activity of the humanized AP201 was similar to that of the parental PG4D2. In addition, AP201 exhibited antitumor and antimetastatic activity against publicly available osteosarcoma cell lines and the newly developed patient-derived osteosarcoma models *in vivo*. These results indicate that PDPN is a promising therapeutic target in osteosarcoma.

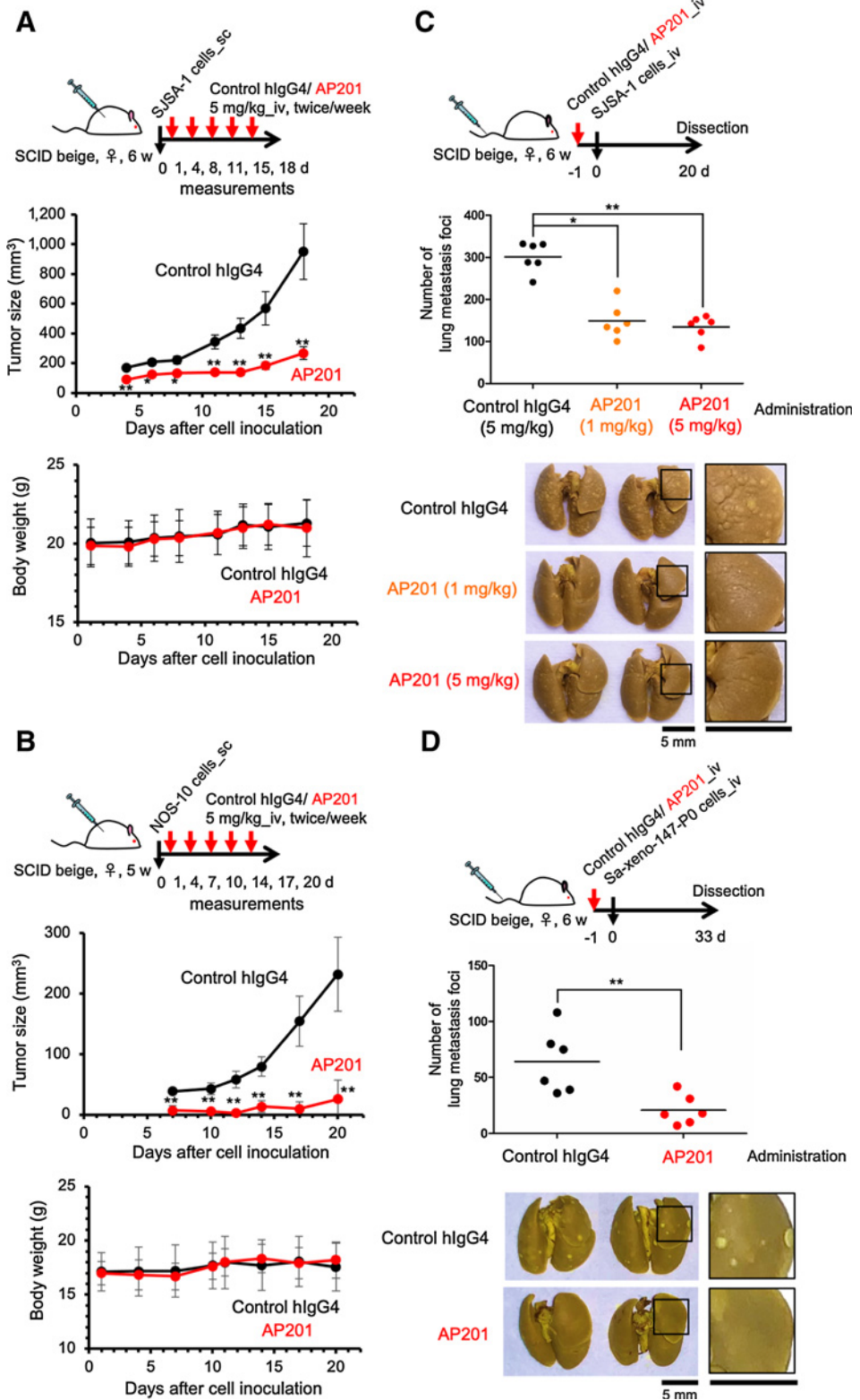
As suggested in some reports (14, 20), the metastasis of PDPN-positive tumor cells relies on PDPN-induced platelet aggregation, possibly through the promotion of a high frequency of tumor cell embolization and the upregulation of invasive ability by PDGFs. In this study, we clearly showed that PDGF released from activated platelets induced the activation of PDGFR α or PDGFR β in osteosarcoma. Thus, PG4D2 and AP201, the neutralizing PDPN antibodies devel-

oped by us, inhibited the growth of PDPN- and PDGFR-positive osteosarcoma cells, such as SJS-1 and NOS-10, *in vivo* and may have suppressed the metastasis of PDPN-positive osteosarcoma by inhibiting PDPN-mediated platelet activation. Previously, we reported that the growth of the PDPN-overexpressing osteosarcoma cell line MG63 was promoted by PDPN-induced platelet activation via the PDGFR β /PI3K/Akt signaling pathway and was partially suppressed by a PDGFR inhibitor (29). In this study, we found that EGFR activation was also associated with the promotion of growth by activated platelets.

In epithelial cancers, such as lung squamous cell carcinoma, platelet-secreted factors such as TGF β , which are released during PDPN-induced platelet aggregation, induce EMT and upregulate invasiveness, which results in longer survival in disseminated tissue owing to extravasation from vessels, leading to metastasis (20). On the other hand, osteosarcoma originates from mesenchymal cells. Thus, the EMT may not contribute to disseminated cell survival in distant organs. However, in our previous report, the migration and invasive activity of osteosarcoma cells were upregulated on coculture with platelets (29). Recently, we found that the release of LPA from activated platelets is a mechanism underlying the promotion of osteosarcoma metastasis by platelet activation (21). Although no correlation between the LPAR1 and PDPN expression levels was observed, some osteosarcoma cells were expressing both LPAR1 and PDPN. Thus, we believe that in high PDPN-expressing osteosarcoma cells, PDPN induces platelet activation that results in LPA release from platelets, and the released LPA might upregulate the migration and invasion activity in those osteosarcoma cells. Considering both our previous results and those of the current study, platelets may play a crucial role in the growth and metastasis of osteosarcoma cells. Thus, inhibition of platelet activation mediated by PDPN might be a promising therapeutic strategy for osteosarcoma; however, further studies are needed to examine whether PDPN expression could be a biomarker to predict the therapeutic efficacy of the anti-PDPN antibody. In addition, studies

Figure 6.

The suppression of PDPN-positive OS xenograft tumor growth and metastasis by humanized anti-PDPN AP201. High PDPN-expressing SJSA-1 (A) or NOS-10 (B) cells were subcutaneously inoculated into mice (5×10^6 or 7.6×10^6 cells/mouse) and treated with AP201 (5 mg/kg) or control human IgG4 (5 mg/kg) twice a week. Tumor size and body weight were measured and the average \pm SD are shown ($n = 6$ or 5). The antimetastatic effects of AP201 on OS metastasis was tested as follows: AP201 (1 or 5 mg/kg for SJSA-1, and 5 mg/kg for Sa-xeno-147-P0) or control human IgG4 (5 mg/kg) was intravenously injected one day before the intravenous injection of SJSA-1 cells (C) or Sa-xeno-147-P0 cells (D); 4×10^5 or 1×10^6 cells/mouse, respectively). After 20 or 33 days, the mice were euthanized, and the lungs were excised. The number of metastatic foci on the lung surface were counted after picric acid staining. The representative pictures of lungs and the magnified image surrounded by boxes are shown [graph demonstrating the number of metastatic foci with averages (bars), top; lung photos, bottom]. Statistical analyses were performed by the Kruskal-Wallis test. *, $P < 0.05$; **, $P < 0.01$. Scale bars, 5 mm.



on whether PDPN overexpression plays similar roles in tumor growth and metastasis through platelet activation in different cancer types are warranted. It is also important to look for effective combination therapies to enhance anti-PDPN antibody treatment

as advanced osteosarcomas often show resistance to chemotherapy. For example, vertical inhibition alone, such as anti-PDPN antibody with PDGFR inhibition in osteosarcomas, or in combination with standard chemotherapy or immunotherapy might be useful because

tumor–platelet interactions play multiple roles in the cancer micro-environment, including in immune escape.

In this study, we developed a humanized anti-PDPN antibody with IgG4 subclass. To develop cells that produce humanized AP201 with high efficiency, we investigated the type of signal peptides fused to the N-terminus of both chains and the expression ratio of the L to H chains. By replacing the original signal peptide with that of Campath-1H and transducing more than double the amount of L chains than H chains into cells, we succeeded in developing a pool of cells with a high antibody production rate. Furthermore, we developed a high antibody-producing cell line by sorting the cells that express AP201 on the cell surface. In the culture process of antibody-producing cells, the concentration and supplements of the basic medium as well as the culture temperature were screened to determine the optimal conditions for antibody production. In the purification process of the antibodies, strict parameters were set for the following steps: clarification filtration, Protein A affinity chromatography, virus inactivation by low pH treatment, two types of ion-exchange chromatography for host-derived protein and DNA removal, virus removal, concentration, and buffer exchange. Finally, we were able to achieve the World Health Organization standard of < 100 ppm of host-derived protein and obtain a high-quality AP201.

We generated AP201 as a human IgG4 subtype antibody that does not exhibit ADCC/CDC activity. The key mechanism of action of the antitumor activity of AP201 is the neutralization of the PDPN–CLEC-2 interaction. Because high-dose AP201 administration did not induce acute toxicity in *Pdpn*^{KI/KI} mice, where a region containing mouse PDPN PLAG4 was converted to a human homologous region, AP201 may be a promising therapeutic agent for osteosarcoma. We reported that the repeated administration of PG4D2 with potent ADCC/CDC activity did not exhibit toxicity or changes in hematologic and biochemical parameters in *Pdpn*^{KI/KI} mice (28). This result suggests that adding ADCC/CDC activity or modification as an antibody–drug conjugate would enhance the efficacy of AP201 therapy.

References

- Biazzo A, De Paolis M. Multidisciplinary approach to osteosarcoma. *Acta Orthop Belg* 2016;82:690–8.
- Sheng G, Gao Y, Yang Y, Wu H. Osteosarcoma and Metastasis. *Front Oncol* 2021;11:780264.
- Lilienthal I, Herold N. Targeting molecular mechanisms underlying treatment efficacy and resistance in osteosarcoma: a review of current and future strategies. *Int J Mol Sci* 2020;21:6885.
- Ariizumi T, Ogose A, Kawashima H, Hotta T, Li G, Xu Y, et al. Expression of podoplanin in human bone and bone tumors: new marker of osteogenic and chondrogenic bone tumors. *Pathol Int* 2010;60:193–202.
- Kunita A, Kashima TG, Ohazama A, Grigoriadis AE, Fukayama M. Podoplanin is regulated by AP-1 and promotes platelet aggregation and cell migration in osteosarcoma. *Am J Pathol* 2011;179:1041–9.
- Kaneko MK, Oki H, Ogasawara S, Takagi M, Kato Y. Anti-podoplanin monoclonal antibody LpMab-7 detects metastatic lesions of osteosarcoma. *Monoclon Antib Immunodiagn Immunother* 2015;34:154–61.
- Wang X, Li W, Bi J, Wang J, Ni L, Shi Q, et al. Association of high PDPN expression with pulmonary metastasis of osteosarcoma and patient prognosis. *Oncol Lett* 2019;18:6323–30.
- Ichikawa J, Ando T, Kawasaki T, Sasaki T, Shirai T, Tsukiji N, et al. Role of platelet C-type lectin-like receptor 2 in promoting lung metastasis in osteosarcoma. *J Bone Miner Res* 2020;35:1738–50.

Authors' Disclosures

N. Fujita reports grants from Japan Agency for Medical Research and Development (AMED), MEXT/JSPS, and Nippon Foundation, and grants and non-financial support from API Co., Ltd. during the conduct of the study; grants from Toppan Printing outside the submitted work; in addition, N. Fujita has a patent for US 10,730,939 B2 issued and a patent for US20210403555A1 pending. No disclosures were reported by the other authors.

Authors' Contributions

A. Takemoto: Conceptualization, resources, investigation, writing–original draft, writing–review and editing. **S. Takagi:** Conceptualization. **T. Ukaji:** Conceptualization, investigation. **N. Gyobu:** Conceptualization, investigation, writing–original draft. **M. Kakino:** Conceptualization, investigation, writing–original draft. **M. Takami:** Resources, investigation. **A. Kobayashi:** Investigation. **M. Lebel:** Investigation. **T. Kawaguchi:** Resources, investigation. **M. Sugawara:** Resources, investigation. **K. Tsuji-Takayama:** Conceptualization, funding acquisition, writing–original draft. **K. Ichihara:** Conceptualization. **Y. Funachi:** Resources. **K. Ae:** Resources. **S. Matsumoto:** Resources. **Y. Sugiura:** Validation, investigation. **K. Takeuchi:** Resources. **T. Noda:** Supervision, resources. **R. Katayama:** Conceptualization, supervision, writing–original draft, writing–review and editing. **N. Fujita:** Conceptualization, supervision, funding acquisition, writing–original draft, writing–review and editing.

Acknowledgments

This study was financially supported by the Project for Cancer Research and Therapeutic Evolution (P-CREATE) grant number 20cm0106205h0005 (to N. Fujita) and the Acceleration Transformative Research for Medical Innovation (ACT-M) grant number 20im0210110h0103 (to N. Fujita) and grant number 20im0210110h0003 (to Api, Co., Ltd.) from the Japan Agency for Medical Research and Development (AMED). This study was also financially supported by MEXT/JSPS KAKENHI grant number JP17H06327 (to N. Fujita) and a grant from the Nippon Foundation (to N. Fujita). The authors acknowledge Nihon Bioresearch Inc (Gifu, Japan) for performing safety study.

The costs of publication of this article were defrayed in part by the payment of page charges. This article must therefore be hereby marked *advertisement* in accordance with 18 U.S.C. Section 1734 solely to indicate this fact.

Received December 21, 2021; revised March 6, 2022; accepted April 1, 2022; published first April 5, 2022.

- Kato Y, Kaneko M, Sata M, Fujita N, Tsuruo T, Osawa M. Enhanced expression of Aggrus (T1alpha/podoplanin), a platelet-aggregation-inducing factor in lung squamous cell carcinoma. *Tumour Biol* 2005;26:195–200.
- Schacht V, Dadras SS, Johnson LA, Jackson DG, Hong YK, Detmar M. Up-regulation of the lymphatic marker podoplanin, a mucin-type transmembrane glycoprotein, in human squamous cell carcinomas and germ cell tumors. *Am J Pathol* 2005;166:913–21.
- Kimura N, Kimura I. Podoplanin as a marker for mesothelioma. *Pathol Int* 2005; 55:83–6.
- Martin-Villar E, Scholl FG, Gamallo C, Yurrita MM, Munoz-Guerra M, Cruces J, et al. Characterization of human PA2.26 antigen (T1alpha-2, podoplanin), a small membrane mucin induced in oral squamous cell carcinomas. *Int J Cancer* 2005;113:899–910.
- Mishima K, Kato Y, Kaneko MK, Nishikawa R, Hirose T, Matsutani M. Increased expression of podoplanin in malignant astrocytic tumors as a novel molecular marker of malignant progression. *Acta Neuropathol* 2006;111:483–8.
- Takagi S, Oh-hara T, Sato S, Gong B, Takami M, Fujita N. Expression of Aggrus/podoplanin in bladder cancer and its role in pulmonary metastasis. *Int J Cancer* 2014;134:2605–14.
- Kato Y, Fujita N, Kunita A, Sato S, Kaneko M, Osawa M, et al. Molecular identification of Aggrus/T1alpha as a platelet aggregation-inducing factor expressed in colorectal tumors. *J Biol Chem* 2003;278:51599–605.

16. Suzuki-Inoue K, Kato Y, Inoue O, Kaneko MK, Mishima K, Yatomi Y, et al. Involvement of the snake toxin receptor CLEC-2, in podoplanin-mediated platelet activation, by cancer cells. *J Biol Chem* 2007;282:25993–6001.
17. Kato Y, Kaneko MK, Kunita A, Ito H, Kameyama A, Ogasawara S, et al. Molecular analysis of the pathophysiological binding of the platelet aggregation-inducing factor podoplanin to the C-type lectin-like receptor CLEC-2. *Cancer Sci* 2008;99:54–61.
18. Suzuki-Inoue K, Fuller GL, Garcia A, Eble JA, Pohlmann S, Inoue O, et al. A novel Syk-dependent mechanism of platelet activation by the C-type lectin receptor CLEC-2. *Blood* 2006;107:542–9.
19. Martin EM, Zuidschewoude M, Moran LA, Di Y, Garcia A, Watson SP. The structure of CLEC-2: mechanisms of dimerization and higher-order clustering. *Platelets* 2021;32:733–43.
20. Takemoto A, Okitaka M, Takagi S, Takami M, Sato S, Nishio M, et al. A critical role of platelet TGF-beta release in podoplanin-mediated tumour invasion and metastasis. *Sci Rep* 2017;7:42186.
21. Takagi S, Sasaki Y, Koike S, Takemoto A, Seto Y, Haraguchi M, et al. Platelet-derived lysophosphatidic acid mediated LPAR1 activation as a therapeutic target for osteosarcoma metastasis. *Oncogene* 2021;40:5548–58.
22. Kaneko MK, Kunita A, Abe S, Tsujimoto Y, Fukayama M, Goto K, et al. Chimeric anti-podoplanin antibody suppresses tumor metastasis through neutralization and antibody-dependent cellular cytotoxicity. *Cancer Sci* 2012;103:1913–9.
23. Nakazawa Y, Takagi S, Sato S, Oh-hara T, Koike S, Takami M, et al. Prevention of hematogenous metastasis by neutralizing mice and its chimeric anti-Aggrus/podoplanin antibodies. *Cancer Sci* 2011;102:2051–7.
24. Takagi S, Sato S, Oh-hara T, Takami M, Koike S, Mishima Y, et al. Platelets promote tumor growth and metastasis via direct interaction between Aggrus/podoplanin and CLEC-2. *PLoS One* 2013;8:e73609.
25. Sekiguchi T, Takemoto A, Takagi S, Takatori K, Sato S, Takami M, et al. Targeting a novel domain in podoplanin for inhibiting platelet-mediated tumor metastasis. *Oncotarget* 2016;7:3934–46.
26. Takemoto A, Miyata K, Fujita N. Platelet-activating factor podoplanin: from discovery to drug development. *Cancer Metastasis Rev* 2017;36:225–34.
27. Miyata K, Takemoto A, Okumura S, Nishio M, Fujita N. Podoplanin enhances lung cancer cell growth *in vivo* by inducing platelet aggregation. *Sci Rep* 2017;7:4059.
28. Ukaji T, Takemoto A, Shibata H, Kakino M, Takagi S, Katayama R, et al. Novel knock-in mouse model for the evaluation of the therapeutic efficacy and toxicity of human podoplanin-targeting agents. *Cancer Sci* 2021;112:2299–313.
29. Takagi S, Takemoto A, Takami M, Oh-Hara T, Fujita N. Platelets promote osteosarcoma cell growth through activation of the platelet-derived growth factor receptor-Akt signaling axis. *Cancer Sci* 2014;105:983–8.
30. Zhang Y, Yang J, Zhao N, Wang C, Kamar S, Zhou Y, et al. Progress in the chemotherapeutic treatment of osteosarcoma. *Oncol Lett* 2018;16:6228–37.
31. Laird AD, Vajkoczy P, Shawver LK, Thurnher A, Liang C, Mohammadi M, et al. SU6668 is a potent antiangiogenic and antitumor agent that induces regression of established tumors. *Cancer Res* 2000;60:4152–60.
32. Roberts WG, Whalen PM, Soderstrom E, Moraski G, Lyssikatos JP, Wang HF, et al. Antiangiogenic and antitumor activity of a selective PDGFR tyrosine kinase inhibitor, CP-673,451. *Cancer Res* 2005;65:957–66.
33. Ukaji T, Takemoto A, Katayama R, Takeuchi K, Fujita N. A safety study of newly generated anti-podoplanin-neutralizing antibody in cynomolgus monkey (*Macaca fascicularis*). *Oncotarget* 2018;9:33322–36.
34. Suzuki-Inoue K, Tsukiji N. Platelet CLEC-2 and lung development. *Res Pract Thromb Haemost* 2020;4:481–90.